Diffusion of glycerol through *Escherichia coli* aquaglyceroporin GlpF

Jérôme Hénin,[*‡] Emad Tajkhorshid,[†] Klaus Schulten,[†] and Christophe Chipot[*]

[*] Equipe de dynamique des assemblages membranaires, UMR CNRS/UHP 7565, Nancy Université, BP 239, 54506 Vandœuvre-lès-Nancy cedex, France; and [†] Theoretical and Computational Biophysics Group, Beckman Institute, University of Illinois at Urbana-Champaign, Urbana, Illinois 61801[§¶]

ABSTRACT   The glycerol uptake facilitator, GlpF, a major intrinsic protein found in *Escherichia coli*, conducts selectively water and glycerol across the inner membrane. The free energy landscape characterizing the assisted transport of glycerol by this homotetrameric aquaglyceroporin has been explored by means of equilibrium molecular dynamics over a time scale spanning 0.12 μs. In order to overcome the free energy barriers of the conduction pathway, an adaptive biasing force (ABF) is applied to the glycerol molecule confined in each of the four channels. The results illuminate the critical role played by intramolecular relaxation on the diffusion properties of the permeant. The present free energy calculations reveal that glycerol tumbles and isomerizes on a time scale comparable to that spanned by its ABF-assisted conduction in GlpF. As a result, reorientation and conformational equilibrium of glycerol in GlpF constitute a bottleneck in the molecular simulations of the permeation event. A profile characterizing the position-dependent diffusion of the permeant has been determined, allowing reaction rate theory to be applied for investigating conduction kinetics based on the measured free energy landscape.

INTRODUCTION

In the course of their evolution, living organisms have learnt to adapt to inhospitable environments by perfecting their cell membrane to become impervious to toxic compounds, while allowing useful, innocuous chemical species to translocate selectively. The physiological processes that regulate the inward transport of water and nutrients across the cell barrier and the outward release of waste material are accomplished by highly specific membrane proteins, among which the family of major intrinsic proteins. The glycerol uptake facilitator (1–3) (GlpF) constitutes a noteworthy member of this family, found among others in *Escherichia coli*. This aquaporin (4), ubiquitous in living organisms, is responsible for passive transport of water and small hydrophilic species, such as linear polyalcohols.

GlpF possesses a homotetrameric structure, each monomer forming an independently functional, 28 Å–long pore. Particularly important elements constituting the core of this protein are two half-membrane spanning repeats related by an essentially two-fold symmetry (3). Approximately half of each repeat is α-helical, the remainder of the scaffold being clearly non-helical. The narrowest section of the pore, known as the selectivity filter (SF), is located roughly 8 Å from the central plane of the lipid bilayer. The N–termini of the α-helical repeats convene roughly at the center of the channel, where the so-called Asn–Pro–Ala (NPA) motifs are located — motifs particularly well conserved among all aquaporins (5). With the high-resolution structures of GlpF at 2.2 Å (6–8) new light

was shed on the sophisticated mechanisms developed by the cell machinery to survive in hostile, nutrient-poor surroundings. In *Escherichia coli*, for instance, glycerol is conveyed in a nonselective fashion across the outer membrane by porins, and then selectively across the inner membrane by aquaglyceroporins, like GlpF. Phosphorylation by glycerol kinase in the cytoplasm traps glycerol in the cell and initiates its consumption, hence, precluding diffusion back through the inner bacterial membrane. Among the remarkable structural features of GlpF, a periplasmic vestibule has been postulated to be conducive to efficient glycerol uptake (9), which promotes rapid bacterial growth in low-concentration glycerol solutions. The 2.2 Å crystallographic structure of GlpF offers an opportunity for elucidating the function of homologous transporters by means of site-directed mutagenesis experiments (10). An improved understanding of the underlying mechanisms that govern water and glycerol conduction in aquaporins is desirable, because these major intrinsic proteins are implicated in critical inherited diseases, such as congenital cataract (11).

Considerable effort has been invested in recent years to decipher the function of aquaporins by means of molecular dynamics (MD) simulations (8, 12–15), in particular the conduction events of glycerol through GlpF (9, 16). Due to the long time scales covered by the slow diffusion of glycerol in GlpF (17), currently not amenable to all-atom MD, investigation of the rare conduction events has been tackled using steered MD (18) (SMD), whereby permeation is accelerated through the application of an external force. Under the appropriate pulling regime, the equilibrium free energy profile across the conduction pathway may be recovered from an ensemble of independent irreversible transformations, employing the

Jarzynski identity (19). Cognizant of the inherent limitations of nonequilibrium simulations to provide a realistic picture of the conformational and orientational relaxation phenomena in transmembrane channels, conduction of glycerol in GlpF was investigated at thermodynamic equilibrium, using an adaptive biasing force (20, 21) (ABF) scheme to overcome the barriers and escape from the minima of the free energy landscape. The simulations reveal that the time scales spanned by the ABF-assisted transport of glycerol and its reorientation and isomerization in GlpF are comparable. The free energy profile averaged over the four different channels is smooth and features a single barrier, the height of which is consistent with experimental observables (17). Based on the free energy profile and the position-dependent diffusion coefficient, diffusional kinetic theory is applied to compute a mean first passage time for glycerol conduction across GlpF.

THEORY AND METHODS

Modeling

Solvation of the GlpF homotetramer in a fully hydrated palmitoyloleylphosphatidyl-ethanolamine (POPE) bilayer is described in reference (16). The choice of POPE as a relevant model of the inner membrane of *Escherichia coli* has been discussed previously (22). As was shown by Jensen *et al.*, the thickness of this membrane model is consistent with the size of the protein (16). In the present work, the z–direction of Cartesian space coincides with the normal to the water-membrane interface. To enhance the statistical information supplied by the simulations, the assisted transport of glycerol was investigated along that spatial direction, in the four channels of GlpF, through the definition of four independent reaction coordinates.

MD simulations

All simulations were performed using the NAMD simulation package (23) in the isobaric-isothermal ensemble. The pressure and the temperature were maintained at 1 bar and 300 K, respectively, employing the Langevin piston algorithm (24) and softly damped Langevin dynamics. The particle-mesh Ewald method (25) was utilized to compute electrostatic interactions. The r–RESPA multiple time-step integrator (26) was used with a time step of 2 fs for short-range and 4 fs for long-range forces. Covalent bonds involving a hydrogen atom were constrained to their equilibrium length. The GlpF homotetramer and its environment were described by the all-atom CHARMM27 force field (27, 28).

ABF free energy calculations

To investigate the assisted transport of glycerol in GlpF, the reaction coordinate was chosen as the distance separating the center of mass of the former from the centroid of the channel in which it was confined, projected onto the z–direction of Cartesian space. Variation of the free energy, $\Delta G(z)$, along z was determined using the ABF method (20), which relies upon the integration of the average force acting on z. In the NAMD implementation of ABF (21), this force is evaluated within the classical thermodynamic integration formalism (29). The free energy derivative, $\mathrm{d}G(z)/\mathrm{d}z$, is estimated locally throughout the simulation, thus providing a continuous update of the biasing force. When applied to the system, this bias generates a Hamiltonian bereft of a net average force along z. Consequently, all values of the reaction coordinate are sampled with an equal probability, thereby improving significantly the accuracy of the computed free energies. To further increase the efficiency of the calculation, the interval connecting the cytoplasmic and the periplasmic sides of the membrane — *viz.* $-20 \leq z \leq +15$ Å, was divided into seven non-overlapping windows, in which up to 30 ns of MD trajectory were generated. The initial Cartesian coordinates of the system for each window were obtained from the constant-velocity (*cv*) SMD simulations of Jensen *et al.* (9), with a preliminary equilibration stage of *ca.* 1 ns. Instantaneous values of the force were accrued in bins 0.1 Å wide, which appears to constitute a reasonable choice for modeling transport phenomena (21). To understand how the measured free energy can be affected by the choice of the reaction coordinate, an alternate definition of the latter was examined, whereby the center of mass of the complete channel was replaced by that of the SF. To this end, a 20 ns ABF simulation was performed using a single, 10–Å broad window embracing the entire free energy barrier that arises between the periplasmic vestibule and the NPA filter. Moreover, increasing the width of the windows constitutes a possible route to fathom quasi non-ergodicity scenarios prone to occur in stratified approaches (30), in particular when the reaction coordinate is strongly coupled to slowly relaxing orthogonal degrees of freedom. Combining the statistical information accrued using both choices of a reaction coordinate, exploration of the reaction pathway characterizing the translocation of glycerol through GlpF was carried over a total simulation time equal to 0.12 μs.

Diffusion coefficient measurements

A set of independent simulations was performed at key positions along the conduction pathway, from which a profile of z-dependent diffusion coefficients, $D(z)$, was computed. A con-

venient, concise expression for $D(z)$ was derived by Hummer in the framework of an overdamped harmonic oscillator (31):

$$D(z) = \frac{\mathrm{var}(z)}{\tau_z} \qquad (1)$$

where the variance, $\mathrm{var}(z)$, is equal to $\langle z^2 \rangle - \langle z \rangle^2$, and τ_z is the characteristic time of the normalized autocorrelation function of z, that is:

$$\tau_z = \frac{\displaystyle\int_0^{+\infty} \langle \delta z(t)\, \delta z(0) \rangle \; \mathrm{d}t}{\mathrm{var}(z)} \qquad (2)$$

Here, $\delta z(t) = z(t) - \langle z \rangle$. The autocorrelation functions were determined from 4-ns MD simulations, during which the vertical position of the glycerol molecules was restrained by means of a harmonic potential with a force constant equal to 10 kcal/mol/Å^2 (21). Each simulation yielded four estimates of $D(z)$, corresponding to distinct positions of the permeant in the four individual channels of GlpF. As a basis of comparison, the effective diffusion coefficient of glycerol in bulk water was estimated from its mean-square displacement measured in an independent, 20-ns simulation.

RESULTS AND DISCUSSION

Free energy of glycerol transport

As revealed in Figure 1, the free energy profile delineating glycerol permeation through GlpF is remarkably simple. The constriction region is prefaced by a shallow vestibular minimum, substantially weaker than that determined from cv–SMD simulations (9). The SF consists of a single free energy barrier, the average height of which, $\Delta G^\ddagger$, is *ca.* 8.7 kcal/mol, falling nicely within the error bar associated to the experimental activation energy of Borgnia and Agre, equal to 9.5±1.5 kcal/mol (17). The remainder of the free energy landscape, in particular near the NPA motif, is essentially flat, hence, suggesting that from this point on, glycerol diffuses rapidly towards the cytoplasm. This result is consistent with previous observations relying on unbiased simulations (16).

In the hypothetical limit of infinite sampling, the free energy profiles delineating the translocation of glycerol in the four different channels of GlpF should superimpose perfectly. Even after 0.12 μs of sampling, this is, however, not completely the case. Whereas the individual potentials of mean force possess identical qualitative features, reaching a fully quantitative agreement constitutes a daunting task. The root mean square deviation (RMSD) of the average force, $\langle F_z \rangle_z$, is, nevertheless,

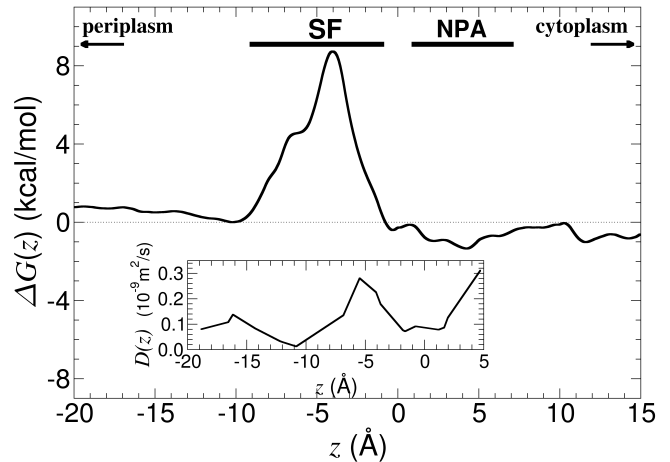
FIGURE 1 Free energy profile for glycerol conduction in the GlpF homotetramer obtained from equilibrium ABF simulations totalling 0.12 μs of sampling, via an integration of the force exerted on glycerol along the z–direction of Cartesian space. This potential of mean force corresponds to an average of the individual free energy profiles determined in the four channels forming GlpF. Inset: z–dependent diffusion of glycerol in GlpF derived from additional simulations, wherein the permeant is confined in a harmonic potential.

moderate and peaks at *ca.* 2.2 kcal/mol/Å in the entropically most challenging region of the conduction pathway, *viz.* its constriction section. This result, together with the qualitative understanding of convergence issues detailed in the following paragraphs, justifies the assertion that convergence of the free energy calculation has been attained.

It is important to underline that throughout the 0.12 μs of ABF simulations, only minute structural differences in GlpF have been detected. The distance RMSD computed over the trace of the different channels never exceeds 2.2 Å. Furthermore, secondary structure analysis (32) does not unveil any unsuspected alteration or loss of structure. On the contrary, over the time scale explored by the present simulations, the entire scaffold of TM α-helices forming the homotetramer remains utterly intact.

Choice of the reaction coordinate and nonequilibrium phenomena

To a large extent, the efficiency of the free energy calculation — albeit, in principle, not its accuracy — depends upon the choice of the reaction coordinate. Ideally, the latter ought to embrace all relevant slow degrees of freedom to guarantee rapidly converging free energy differences (33). In practice, however, efficiency of the calculation collapses when diffusion along the reaction pathway follows narrow valleys separated by high free energy barriers.

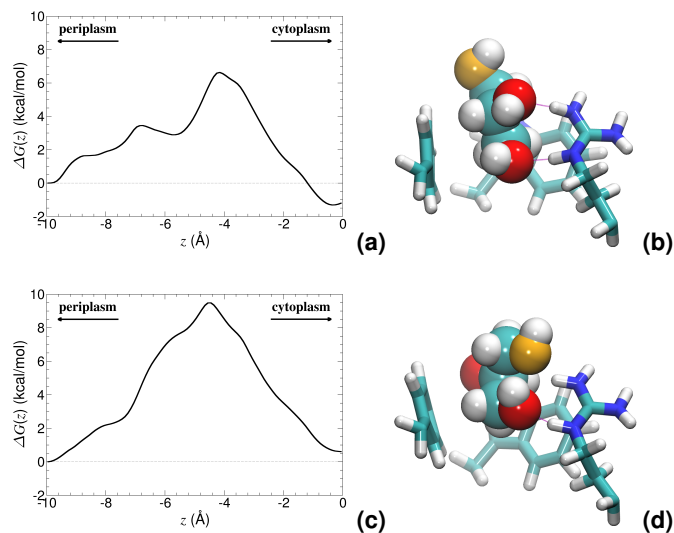This shortcoming is further magnified in the event of a subopti-

FIGURE 2 Energetics deduced from incomplete sampling of glycerol transport across the SF region of GlpF. One trajectory captures a local minimum (**a**) mirrored in a typical conformation of the permeant (**b**). Another trajectory samples a monolithic barrier (**c**) corresponding to an inadequate orientation and conformation of glycerol (**d**). Image rendering was done with VMD (34).

mal selection of the reaction coordinate, incapable of mirroring the intricate topology of the molecular system. Whereas, in an average sense, the normal to the water-membrane interface — *i.e.* the z–direction of Cartesian space, constitutes a natural choice for modeling the permeation of glycerol in GlpF, well-localized distortions in the conduit demonstrate that a surrogate, one-dimensional reaction coordinate may not be able to capture fully the motion of the permeant as it crawls through the crooked and narrow regions of the channel. In particular, markedly different behaviors have been monitored between consecutive passages of glycerol at given heights of the channel, even though the time elapsed between these passages can span several nanoseconds. As illustrated in Figure 2, local deviations of the pathway with respect to a hypothetically straight hollow tubular structure causes glycerol to collide against the walls of the SF. Alteration of the latter through isomerization of the participating amino acids may be viewed as the result of quasi nonequilibrium effects, which are likely to be rooted in the application of the adaptive bias before the estimate of the average force is properly converged. The permeant is then thrusted artificially towards the edge of the channel, only because the choice of the reaction coordinate is locally inadequate. Although a one-dimensional description is formally correct, convergence of the free energy calculation can be severely impeded by quasi nonequilibrium phenomena requiring much longer sampling times to allow closely coupled, slow degrees of freedom to relax appropriately.

Orientation and conformational equilibrium of glycerol

At the experimental level, the activation energy measured for glycerol conduction through GlpF (17) involves an average over an ensemble of molecules entering the constriction region of the aquaglyceroporin with distinct conformations and orientations. On the time scale of the experiment, it is expected that glycerol reorients to optimize its induced fit in the SF and NPA regions, the exploration of which may be hardly amenable to equilibrium free energy calculations — and even less so to irreversible pulling simulations (35). A closer look at the four permeant molecules as they enter the SF sheds new light on the intimate relationship between orientation, isomerization, and free energy. From the latter, it may be understood that exaggeratingly short free energy calculations starting with a quasi-optimal orientation and conformation of glycerol may reflect artificially an unhampered diffusion and the disappearance of the free energy barrier.
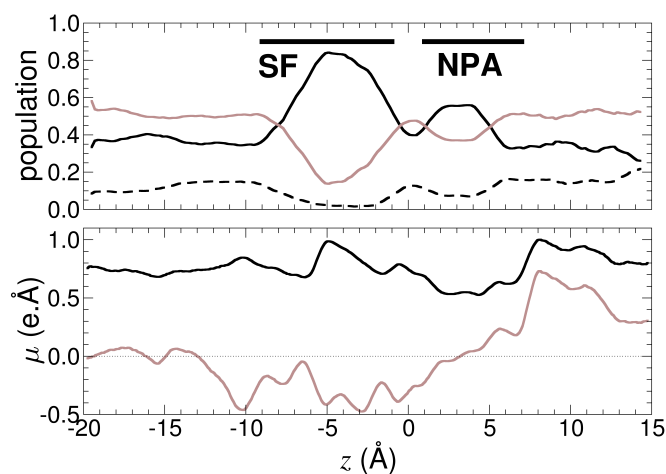

FIGURE 3 Top: Conformational and orientational preference of glycerol in the GlpF homotetramer, as a function of the reaction coordinate, z: Population of *gauche-gauche* (dark, solid line), *gauche-anti* (light, solid line) and *anti-anti* (dark, dashed line) conformations. Bottom: Total molecular dipole moment of glycerol (dark, solid line) and its projection along the z–direction of Cartesian space (light, solid line), averaged over the four channels of GlpF.

Analysis of the MD trajectories indicate that, when confined in the conduction pathway, glycerol may isomerize and adopt three possible conformations — *viz. gauche-gauche*, *gauche-anti* and *anti-anti*, as labeled after the configuration of the two O–C–C–O torsional angles. As indicated in Figure 3, the relative population of these conformers varies dramatically as a function of the position of glycerol in the channel. In bulk water, the *anti-anti* conformation is stabilized by an intramolecular hydrogen bond, whereas the two other, more compact forms are predominant inside the constriction region of the channel. In the SF, the *gauche-gauche* conformation is preferred

because it promotes the formation of a network of hydrogen bonds with the neighboring Phe[200] and Arg[206] residues, as shown in Figures 4 and 5, while the non-polar face of the molecule forms favorable hydrophobic contacts with the side chains of Trp[48] and Phe[200]. In the same region, the *anti-anti* conformer is the least populated on account of the lesser possibilities offered for hydrogen-bonded motifs.
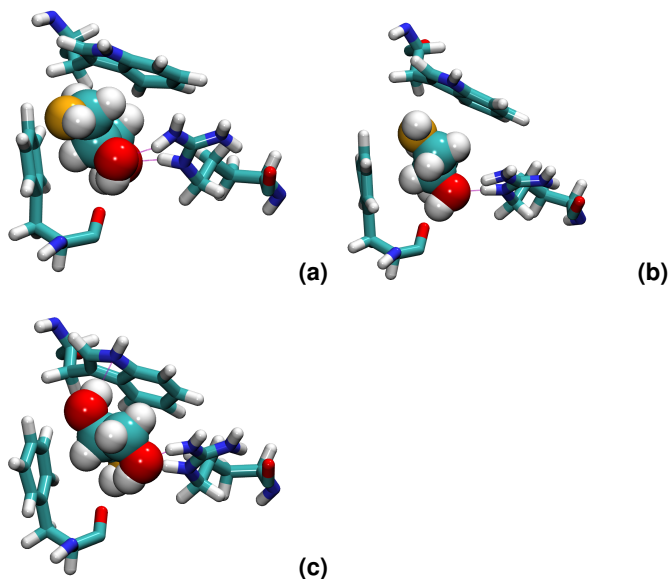

(a)   **(b)**

(c)

FIGURE 4 Conformational equilibrium of glycerol in the SF region of the GlpF homotetramer: *gauche–gauche* (**a**), *gauche–anti* (**b**) and *anti–anti* (**c**) conformations. Image rendering was done with VMD (34).

Orientation of glycerol in the midst of the SF follows a two-state regime, whereby the vector joining the first and the last carbon of the molecule is either parallel or antiparallel to the normal to the water-membrane interface, $\hat{n}$. Noteworthily, the preferred parallel orientation is conducive to the emergence of the *gauche-gauche* conformer, hence, suggesting an intimate relationship between orientation and conformation. The marked propensity towards *gauche-anti* conformers for antiparallel orientations further illustrates the stereoselectivity of the channel, in which conformation is dictated by prochirality, as depicted in Figures 3 and 4. Interestingly enough, the average orientation of the dipole moment, μ, obeys a mechanism reminiscent of water transport in GlpF, wherein μ is roughly antiparallel to $\hat{n}$, before tilting to a parallel orientation near the NPA motif (14). Unlike water, however, inversion of the glycerol dipole moment is not strictly correlated with tumbling of the molecule, as it can happen through overall conformational changes and reorientation of individual hydroxyl groups. In addition to the specific interactions with pore-lining residues mentioned previously, this electrostatic effect, thus, introduces another type of coupling between the permeation process and the internal degrees of freedom of the permeant. Both mecha-

nisms are likely to affect the permeation kinetics.

Capturing relaxation phenomena

SMD simulations associated with the Jarzynski identity (19), whereby a permeant molecule is pulled irreversibly in each monomer of GlpF, yield a rugged free energy landscape (9), at variance with the smooth profiles depicted in Figure 1. This marked discrepancy may be explained, at least in part, by the nonequilibrium nature of pulling experiments that do not allow the mutual adaptation of glycerol and the channel as the former is dragged along the conduction pathway. Of particular interest, the two peaks characteristic of the SF in the SMD simulations (9) merge into a single free energy barrier when turning to the ABF approach. This coalescence is likely to be rooted in the ensemble average over all possible orientations of glycerol in equilibrium free energy calculations — which does not favor any particular low-entropy arrangement in the SF. In sharp contrast, glycerol molecules are pre-oriented in irreversible pulling experiments, thereby mirroring the crystallographic structure and forming the expected hydrogen-bonding patterns.
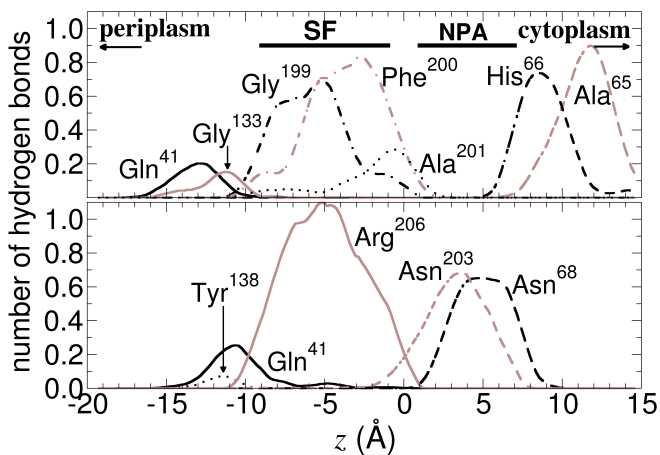

FIGURE 5 Evolution of the number of hydrogen bonds as a function of the reaction coordinate, z. Top: Hydrogen-bond acceptors, bottom: hydrogen-bond donors. Asn[68] and Asn[203] belong to the NPA motif. Arg[206] is able to form two hydrogen bonds simultaneously, hence an average number greater than unity.

In vivo, permeation of GlpF by one glycerol molecule seems to occur at least on the microsecond time scale (1), which precludes a full sampling of the permeation pathway by means of unbiased atomistic simulations. Such a rare event may, nonetheless, be modeled by accelerating the natural process to a time scale compatible with the contingencies of MD-related approaches. Beyond the underlying principles of the methods, the present ABF simulations differ from previous computational investigations in regard to the significantly longer time

scales they cover. As illustrated in Figure 6, isomerization of the permeant in the channel occurs on the multi-nanosecond time scale, flipping of the two torsional angles, φ_1 and φ_2, of glycerol being concerted. This phenomenon spans a somewhat shorter, yet appreciable time scale when glycerol is immersed in bulk water. The absence of concerted transitions in the aqueous environment suggests that coupling of the two angles in the SF of GlpF stems from conformational restrictions in that region. Similarly, reorientation of the permeant — see Figure 6 (c) and (d) — is reasonably fast near the cytoplasm, but is slowed down dramatically in the SF region, where it may remain frozen, either parallel or antiparallel to $\hat{n}$, for as long as *ca.* 10 ns. Pulling experiments of glycerol at the constant velocity of 30 Å/ns are probably not able to capture relaxation phenomena that embrace significantly longer time scales.

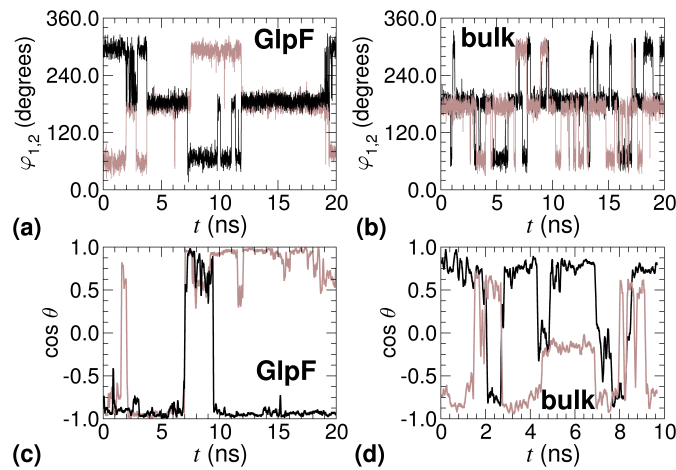
(a)

(b)

(c)

(d)

FIGURE 6 Conformational and orientational relaxation of glycerol in the GlpF homotetramer: Time-evolution of the two torsional angles of glycerol confined in the SF (**a**) and in bulk water (**b**). Time-evolution of the orientation of glycerol in the periplasmic vestibule (**c**) and in the SF (**d**) — monomer 1 (dark, solid line) *vs.* monomer 2 (light, solid line).

Concurrent isomerization and reorientation of glycerol appears to act as the rate-limiting step towards permeation across GlpF. This concerted adaptation to the rough surface of the SF may be related to an induced fit in protein-ligand association. Similar in spirit to the exploration of conformational space by the ligand trying to find its way to the binding pocket, where it will be locked tightly, the permeant searches among all possible combinations of conformation and orientation, for the particular one that will ensure passage through the SF. As glycerol slowly diffuses within the SF region, it is progressively stabilized by the formation of intermolecular hydrogen bonds with the channel. This is illustrated in the movie provided as supplementary material.

Intrinsic dynamics of glycerol and kinetics of permeation

Transport of glycerol in GlpF may be viewed as a diffusion process in an external potential of mean force created by the confined environment of the membrane channels. ABF reshapes the free energy landscape seen by glycerol as it progresses along z, removing kinetic traps and barriers, while keeping a quantitative account of these features. Application of the method requires one to choose an arbitrary parameter, z, as an *a priori* reaction coordinate, though ABF permits the permeant and the channel to adapt mutually as the former moves along z, conferring to the system significant freedom to find the actual reaction pathway. Convergence of the ABF calculation is optimal in the ideal case of a process involving a concerted motion coupling z to other degrees of freedom, with a single, slow degree of freedom, *i.e.* the ABF reaction coordinate, and a fast-relaxing orthogonal manifold. The ABF treatment is perfectly adapted to the reaction rate theory, which relies on this type of time-scale separation — *viz.* the slow manifold being described explicitly, and the fast manifold being introduced as a mean field, in the form of the free energy profile.

The simulations of glycerol in a bulk aqueous environment yield an isotropic diffusion coefficient equal to 2.1×10^{-9} m²/s, in reasonable agreement with the experimental value of 1.1×10^{-9} m²/s determined at 298 K (36). Estimation of a position-dependent diffusion coefficient for the complex motion of glycerol in the confined environment of the channel is far more challenging. Lu *et al.* (37) report an attempt at measuring the diffusion coefficient of glycerol in GlpF based on the velocity autocorrelation functions. This approach yields a value of 2.2×10^{-9} m²/s, a somewhat unrealistic value considering that it is larger than the experimental estimate for glycerol in bulk water (36). Lu *et al.* concluded that long-, nanosecond time-scale sampling is required to quantify self-correlations of the fluctuations that drive glycerol diffusion in the channel. Indeed, as shown in Figure 1, 4-ns measurements based on position autocorrelation functions yield values of the expected order of magnitude, slightly smaller than the diffusion coefficient for water in the same channel, determined by Tajkhorshid *et al.* (8) to be 4.6×10^{-10} m²/s.

It is remarkable that some of the highest values of $D(z)$ within the channel are found in the region of the SF. Tight restrictions on the shape and orientation of glycerol in that highly constricted region (see Figure 3 and discussion above) have the opposing effects of (i) smoothing locally the effective free energy surface — hence, the higher diffusion coefficient, and (ii) imposing a high entropic penalty, thereby reducing significantly the thermal accessibility of that section of the channel.

Not too surprisingly, the second effect is predominant, so that the SF acts, indeed, as a barrier to glycerol permeation, as will be seen below.

The intrinsic diffusion coefficient may be used together with the free energy profile along the reaction pathway to infer the mean first passage time, $\tau(a \rightarrow b)$, of glycerol from the periplasmic vestibule, a, to the cytoplasm, b (38):

$$
\begin{aligned}
\tau(a \rightarrow b) \quad = \quad & \int_a^b \exp[\beta \Delta G(z)] \, D^{-1}(z) \\
\times \quad & \left[\int_a^z \exp[-\beta \Delta G(\zeta)] \, \mathrm{d}\zeta \right] \, \mathrm{d}z \qquad (3)
\end{aligned}
$$

Here $\beta = (k_B T)^{-1}$, where k_B is the Boltzmann constant, T is temperature, and $D(z)$ is the z–dependent diffusion coefficient. As can be seen in Figure 1, the latter varies between *ca.* 0.02 and 0.3×10^{-9} m^2/s — *i.e.* ten to a hundred times slower than the free diffusion of glycerol in an aqueous medium. The noteworthy fast diffusion in the region of the SF confirms that rare events are *rare*, indeed, only because they occur after numerous failed attempts to overcome the free energy barrier — not because climbing the latter is slow (39,40).

Applying Equation 3 to the free energy and the position-dependent diffusion coefficient profiles of Figure 1, it follows that $\tau(a \rightarrow b) = 5 \times 10^{-4}$s — which corresponds to a rate constant of *ca.* 2×10^3 s^{-1}. This rate constant is about two orders of magnitude smaller than the per-channel turnover estimated by Heller *et al.* (1) based on the *in vivo* measurements by Alemohammad and Knowles (41). The theoretical estimates of Lu *et al.* (37), which account for the whole transport process from the periplasm to the cytoplasm, range from 4×10^5 to 10^6 s^{-1}, assuming a 0.5 M glycerol concentration.

CONCLUSION

Glycerol conduction in GlpF has been investigated from the perspective of unprecedented equilibrium free energy calculations executed over a time scale spanning 0.12 μs. Compared to shorter, irreversible pulling experiments, the length of these simulations and their reversible character allow the permeant to reorient and isomerize freely as it diffuses slowly through the conduction pathway. They further illuminate that orientational and conformational relaxation of glycerol and its ABF-assisted transport along the tripathic channels span comparable time scales. The structure of the free energy profile characterizing GlpF permeation by glycerol is qualitatively simple and features a single free energy barrier located at the SF. The height of the free energy barrier separating the periplas-

mic vestibule from the NPA motif, initially modulated by the original orientation of glycerol in the channel, converges after appropriate sampling towards the experimentally determined activation energy (17). In this respect, the present free energy calculations constitute an important, albeit still incomplete step towards the full understanding of glycerol diffusion in GlpF. Of particular interest are the symptomatic quasi nonequilibrium effects that modulate the height of the free energy barrier in the SF region and can be ascribed to both the choice of the reaction coordinate and the convergence of the adaptive bias. The present results imply that conduction in aquaglyceroporins does not exhibit complete time-scale separation, but rather depends on fluctuations that are slow compared with the motion along the conduction pathway. Gating of membrane channels generally obeys such a reaction mechanism. Advancing our understanding of assisted transport phenomena across membranes necessarily requires better characterization of the slow fluctuations that are coupled to self-diffusion in aquaporins and other channels. Application of diffusional kinetic theory based on the measured free energy profile and position-dependent diffusion coefficient yields a predicted rate constant that appears to be overestimated compared to available experimental value. Although the latter relies upon arguable assumptions and only provides a rough idea of the associated kinetics, the present apparent discrepancy calls for additional investigations. Extending the present approach to other transport phenomena, well-characterized experimentally, is envisioned to help assess whether mean-field models — *viz.* diffusion in a one-dimensional potential of mean force — describe in a reliable and effective way the statistical distribution of the permeation events that underlie the observable, macroscopic transport rate.

REFERENCES

1. Heller, K. B., E. C. Lin, and T. H. Wilson. 1980. Substrate specificity and transport properties of the glycerol facilitator of *E*scherichia coli *J. Bacteriol.* 144(1):274–278.

2. Stroud, R. M., P. Nollert, and L. Miercke. 2003. The glycerol facilitator GlpF, its aquaporin family of channels, and their selectivity *Adv. Protein Chem.* 63:291–316.

3. Stroud, R. M., L. J. W. Miercke, J. O'Connell, S. Khademi, J. K. Lee, J. Remis, W. Harries, Y. Robles, and D. Akhavan. 2003. Glycerol facilitator GlpF and the associated aquaporin family of channels *Curr. Opin. Struct. Biol.* 13:424–431.

4. Agre, P., M. Bonhivers, and M. J. Borgnia. 1998. The aquaporins, blueprints for cellular plumbing systems *J. Biol. Chem.* 273(24):14659–14662.

5. Borgnia, M., S. Nielsen, A. Engel, and P. Agre. 1999. Cellular and molecular biology of the aquaporin water channels *Annu. Rev. Biochem.* 68:425–458.

6. Fu, D., A. Libson, L. J. Miercke, C. Weitzman, P. Nollert, J. Krucinski, and R. M. Stroud. 2000. Structure of a glycerol-conducting channel and the basis for its selectivity. *Science* 290(5491):481–6.

7. Nollert, P., W. E. Harries, D. Fu, L. J. Miercke, and R. M. Stroud. 2001. Atomic structure of a glycerol channel and implications for substrate permeation in aqua(glycero)porins *FEBS Lett.* 504:112–7.

8. Tajkhorshid, E., P. Nollert, M. Ø. Jensen, L. J. W. Miercke, J. O'Connell, R. M. Stroud, and K. Schulten. 2002. Control of the selectivity of the aquaporin water channel family by global orientational tuning *Science* 296(5567):525–530.

9. Jensen, M. Ø., S. Park, E. Tajkhorshid, and K. Schulten. 2002. Energetics of glycerol conduction through aquaglyceroporin GlpF *Proc. Natl. Acad. Sci. USA* 99:6731–6736.

10. Lee, J. K., S. K., W. Harries, D. Savage, L. Miercke, and R. M. Stroud. 2004. Water and glycerol permeation through the glycerol channel GlpF and the aquaporin family *J. Synchrotron Radiat.* 11:86–88.

11. Francis, P., V. Berry, S. Bhattacharya, and A. Moore. 2000. Congenital progressive polymorphic cataract caused by a mutation in the major intrinsic protein of the lens, MIP (AQP0) *Br. J. Ophthalmol.* 84(12):1376–1379.

12. de Groot, B. L. and H. Grubmüller. 2001. Water permeation across biological membranes: Mechanism and dynamics of aquaporin–1 and GlpF *Science* 294(5550):2353–2357.

13. Law, R. J. and M. S. P. Sansom. 2004. Homology modelling and molecular dynamics simulations: Comparative studies of human aquaporin-1. *Eur. Biophys. J.* 33:477–489.

14. Wang, Y., K. Schulten, and E. Tajkhorshid. 2005. What makes an aquaporin a glycerol channel? A comparative study of AqpZ and GlpF. *Structure* 13:1107–1118.

15. Patargias, G., P. J. Bond, S. S. Deol, and M. S. P. Sansom. 2005. Molecular dynamics simulations of GlpF in a micelle vs in a bilayer: Conformational dynamics of a membrane protein as a function of environment *J. Phys. Chem. B* 109:575–582.

16. Jensen, M. O., E. Tajkhorshid, and K. Schulten. 2001. The mechanism of glycerol conduction in aquaglyceroporins *Structure* 9(11):1083–1093.

17. Borgnia, M. J. and P. Agre. 2001. Reconstitution and functional comparison of purified GlpF and AqpZ, the glycerol and water channels from *Escherichia coli Proc. Natl. Acad. Sci. USA* 98(5):2888–2893.

18. Izrailev, S., S. Stepaniants, B. Isralewitz, D. Kosztin, H. Lu, F. Molnar, W. Wriggers, and K. Schulten. 1998. Steered molecular dynamics, in *Computational molecular dynamics: Challenges, methods, ideas*, eds. Deuflhard, P., J. Hermans, B. Leimkuhler, A. E. Mark, R. Skeel, and S. Reich. (Springer Verlag, Berlin), Vol 4 of *Lecture Notes in Computational Science and Engineering*, pp. 39–65.

19. Jarzynski, C. 1997. Nonequilibrium equality for free energy differences *Phys. Rev. Lett.* 78:2690–2693.

20. Darve, E. and A. Pohorille. 2001. Calculating free energies using average force *J. Chem. Phys.* 115:9169–9183.

21. Hénin, J. and C. Chipot. 2004. Overcoming free energy barriers using unconstrained molecular dynamics simulations *J. Chem. Phys.* 121:2904–2914.

22. Tieleman, D. P., L. R. Forrest, Sansom M. S. P., and H. J. C. Berendsen. 1998. Lipid properties and the orientation of aromatic residues in OmpF, Influenza M2 and alamethicin systems: Molecular dynamics simulations *Biochemistry* 37:17544–17561.

23. Phillips, J. C., R. Braun, W. Wang, J. Gumbart, E. Tajkhorshid, E. Villa, C. Chipot, L. Skeel, R. D. Kalé, and K. Schulten. 2005. Scalable molecular dynamics with NAMD *J. Comput. Chem.* 26:1781–1802.

24. Feller, S. E., Y. H. Zhang, R. W. Pastor, and B. R Brooks. 1995. Constant pressure molecular dynamics simulations — The Langevin piston method *J. Chem. Phys.* 103:4613–4621.

25. Darden, T. A., D. M. York, and L. G. Pedersen. 1993. Particle mesh Ewald: An $NlogN$ method for ewald sums in large systems *J. Chem. Phys.* 98:10089–10092.

26. Tuckerman, M. E., B. J. Berne, and G. J. Martyna. 1992. Reversible multiple time scale molecular dynamics *J. Phys. Chem. B* 97:1990–2001.

27. MacKerell Jr., A. D., D. Bashford, M. Bellott, R. L. Dunbrack Jr., J. D. Evanseck, M. J. Field, S. Fischer, J. Gao, H. Guo, S. Ha, D. Joseph-McCarthy, L. Kuchnir, K. Kuczera, F. T. K. Lau, C. Mattos, S. Michnick, T. Ngo, D. T. Nguyen, B. Prodhom, W. E. Reiher III, B. Roux, M. Schlenkrich, J. C. Smith, R. Stote, J. Straub, M. Watanabe, J. Wiórkiewicz-Kuczera, D. Yin, and M. Karplus. 1998. All–atom empirical potential for molecular modeling and dynamics studies of proteins *J. Phys. Chem. B* 102:3586–3616.

28. Feller, S. E. and A. D. MacKerell Jr.. 2000. An improved empirical potential energy function for molecular simulations of phospholipids *J. Phys. Chem. B* 104:7510–7515.

29. den Otter, W. K. 2000. Thermodynamic integration of the free energy along a reaction coordinate in Cartesian coordinates *J. Chem. Phys.* 112:7283–7292.

30. Chipot, C. and J. Hénin. 2005. Exploring the free energy landscape of a short peptide using an average force *J. Chem. Phys.* 123:244906.

31. Hummer, G. 2005. Position-dependent diffusion coefficients and free energies from Bayesian analysis of equilibrium and replica molecular dynamics simulations *New J. Phys.* 7:34.

32. Frishman, D. and P. Argos. 1995. Knowledge–based protein secondary structure assignment *Proteins* 23(4):566–579.

33. eds. Chipot, C. and A. Pohorille. *Free energy calculations. Theory and applications in chemistry and biology*, Springer Verlag.

34. Humphrey, W., A. Dalke, and K. Schulten. 1996. VMD — Visual molecular dynamics *J. Molec. Graphics* 14:33–38.

35. Park, S., F. Khalili-Araghi, E. Tajkhorshid, and K. Schulten. 2003. Free energy calculation from steered molecular dynamics simulations using Jarzynski's equality *J. Chem. Phys.* 119:3559–3566.

36. ed. Lide, D. R. *CRC Handbook of Chemistry and Physics, 80th edition*, Chapman and Hall, CRC Press Boca Raton.

37. Lu, D. Y., P. Grayson, and K. Schulten. 2003. Glycerol conductance and physical asymmetry of the *Escherichia coli* glycerol facilitator GlpF *Biophys. J.* 85(5):2977–2987.

38. Szabo, A., K. Schulten, and Z. Schulten. 1980. First passage time approach to diffusion controlled reactions *J. Chem. Phys.* 72:4350–4357.

39. E, W., W. Ren, and E. Vanden-Eijnden. 2005. Transition pathways in complex systems: Reaction coordinates, isocommittor surfaces, and transition tubes *Chemical Physics Letters* 413:242–247.

40. Dellago, C. and G. Hummer. 2006. Kinetics and mechanism of proton transport across membrane nanopores *Phys. Rev. Lett.* 97:245901.

41. Alemohammad, M. M. and C. J. Knowles. 1974. Osmotically induced volume and turbidity changes of *E*scherichia coli due to salts, sucrose and glycerol, with particular reference to the rapid permeation of glycerol into the cell *J. Gen. Microbiol.* 82(1):125–142.